A Mechanistic Dichotomy in the Reactions of $Cp_2M(CH_2{=}CHMe)$ (M = Nb, Ta) with Catecholborane: Generation of Boryl Complexes by Propylene Hydroboration and Propylene Loss

Dean R. Lantero, Susanne L. Miller, Jian-Yang Cho, Donald L. Ward,† and Milton R. Smith III*

Department of Chemistry, Michigan State University, East Lansing, Michigan 48824

Received November 6, 1998

A mixture of *endo*- and *exo*-$Cp_2TaH(CH_2{=}CHMe)$ (**1a**) and catecholborane (HBCat, Cat = 1,2-$O_2C_6H_4$) reacted to give *endo*-$Cp_2TaH_2(BCat)$ (**2a**) and *n*-PrBCat as the major products. Small quantities of *exo*-**2a** are also formed during the reaction. When the reaction was monitored by ^1H NMR, the resonances for *endo*-**1a** were diminished relative to *exo*-**1a**, and eventually all of the olefin complex was consumed. The analogous reaction employing DBCat led to deuterium incorporation at the α-methylene position of *n*-PrBCat and the deuteride positions of **2a**. The alkylborane and deuteride resonances in the ^2H NMR spectrum integrated in a 40:60 ratio. ^1H NMR spectra indicate the α-methylene integration in *n*-PrBCat-d_{0-1} is depleted by 50% of its normal value. A mechanism involving borane attack on a propylidene hydride intermediate is invoked to account for the labeling results. A mixture of *endo*- and *exo*-$Cp_2NbH(CH_2{=}CHMe)$ (**1b**) reacts with HBCat to generate *n*-PrBCat, propane, propylene, Cp_2NbH_2BCat (**2b**), and $Cp_2NbH(BCat)_2$ (**3**). The Markovnikov hydroboration product, *i*-PrBCat was not detected. $Cp_2NbH(BCat)_2$ was isolated as lemon-yellow crystals in 21% yield by fractional crystallization from toluene. ^1H NMR indicates inequivalent boryl environments in compound **3**, and two distinct boron resonances at δ 65 ($\Delta\nu_{1/2}$ = 250 Hz) and δ 60 ($\Delta\nu_{1/2}$ = 210 Hz) were resolved in the ^{11}B NMR spectrum (C_6D_6, 60 °C). $^1H\{^{11}B\}$ spectra and isotopic labeling experiments indicated coupling between the niobium hydride and the ^{11}B resonance at δ 60. Reaction of **1b** with DBCat gave **2b**-d_2, **3**-*d*, propane-d_{0-2} and *n*-PrBCat-d_{0-2}. The deuteride resonance in **3**-*d* is shifted to higher field by 180 ppb relative to the hydride shift in compound **3**. The chemical shift of the hydride resonance in compound **3** was temperature independent between −80 and 25 °C (THF-d_8).Compound **3** was crystallized as a yellow acetone solvate, and its molecular structure was determined. The Nb center lies on a C_2 axis, and the chemically inequivalent boryl groups are symmetry related. An Nb−B distance of 2.29(1) Å was found for compound **3**, and the hydride position could not be reliably located. At low temperature the reaction between *exo*- and *endo*-**1b** with HBCat generates a persistent intermediate, **4**, as the major Cp-containing component. ^1H NMR spectra indicated two new hydride resonances reaction δ −4.40 and δ −6.00, and $^1H\{^{11}B\}$ spectra demonstrated that the resonance at δ −6.00 is coupled to boron. A NOESY spectrum revealed a cross-peak between the two hydride positions of intermediate **4**. Generation of **4**-d_1 from DBCat and *exo*- and *endo*-**1b** proved that the hydride resonance at δ −6.00 arises from the borane. The deuteride resonance in **4**-*d* is shifted to higher field by 210 ppb relative to the hydride shift in compound **4**. A modest temperature dependence for the hydride chemical shifts was observed between −50 and 50 °C (toluene-d_8). Intermediate **4** isomerizes to *endo*-**2b**, and reacts with CO (100 psi at 25 °C) to give the carbonyl compound, $Cp_2NbH(CO)$, and HBCat. Small quantities of intermediate **4** could be generated by heating a solution of *endo*-**2b**. An equilibrium constant could not be accurately determined. On the basis of spectroscopic data and chemical reactivity, the structure *exo*-$Cp_2NbH(\eta^2\text{-}HBCat)$ was assigned to intermediate **4**.

Introduction

Recent interest in reactions between B−H and B−B bonds with transition-metal olefin complexes have stemmed from the potential for discovering new B−C bond forming reactions,[1−8] applications in catalyst design for olefin polymerization,[7,9] and use of the olefin as leaving group for preparing molecules with M−B interactions.[10−12] With the latter goal in mind, we

---

† Author to whom crystallographic correspondence should be addressed.

(1) A comprehensive review of metal-catalyzed hydroboration reactions covering the literature from 1991 to 1997 has recently appeared: Beletskaya, I.; Pelter, A. *Tetrahedron* **1997**, *53*, 4957−5026.

10.1021/om980908m CCC: $18.00 © 1999 American Chemical Society
Publication on Web 12/29/1998

Scheme 1

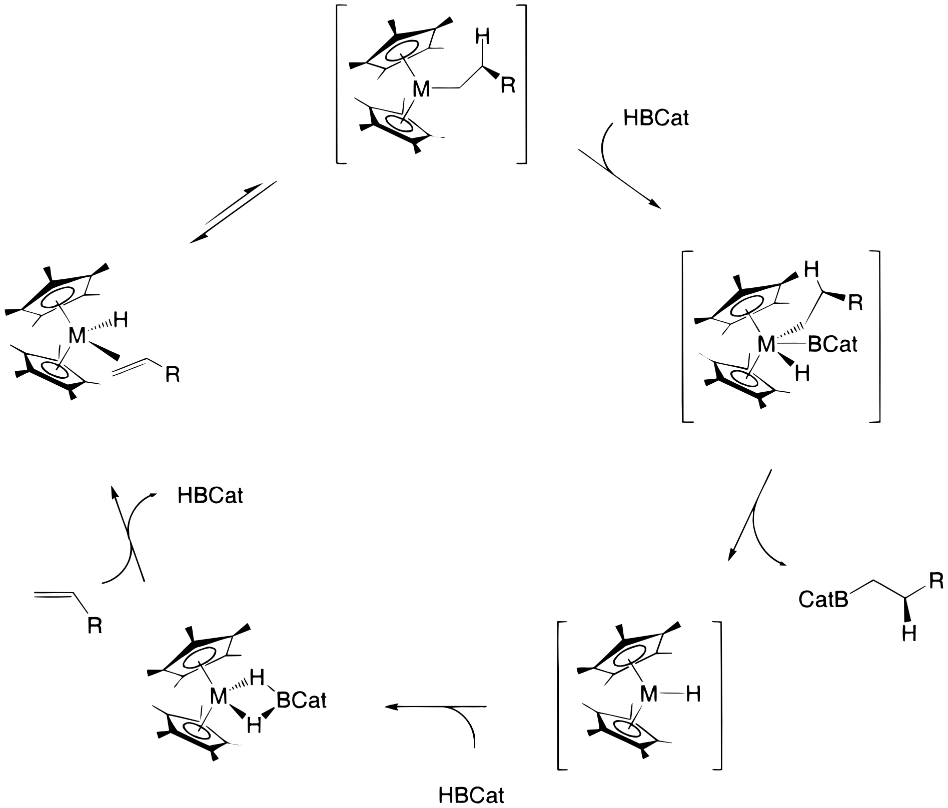

recently found that the olefin complexes *endo*-Cp*$_2$MH(CH$_2$═CHMe) (Cp* = C$_5$Me$_5$, M = Nb, Ta) react with HBCat to generate metal complexes with the formulas *endo*-Cp*$_2$MH$_2$BCat and the olefin hydroboration product *n*-PrBCat.[12,13] Isotopic labeling experiments supported a mechanism that invoked B−H activation by 16-electron alkyl intermediates as outlined in Scheme 1.

The H$_2$BCat moieties in *endo*-Cp*$_2$MH$_2$BCat exhibit fundamentally distinct, metal-dependent binding modes. For example, *endo*-Cp*$_2$TaH$_2$(BCat) is best described as a Ta^{V} boryl complex; whereas, the Nb analogue more closely resembles an HBCat adduct of "Cp*$_2$Nb^{III}H".[14] The differences in ground-state structures correlate with reactivity. For example, facile borane elimination from the Nb compound at ambient temperature makes this system catalytically viable for olefin hydroboration, while the Ta boryl complex eliminates borane slowly at elevated temperatures.[15]

Preparation of the aforementioned Cp* compounds from olefin complexes differs from established routes to Cp$_2$MH$_2$BCat (Cp = C$_5$H$_5$, M = Nb, Ta). Approaches that have succeeded in Cp systems, such as reactions of metallocene trihydrides with HBCat,[16] or reactions of metal anions with haloboranes,[17] failed to give tractable products for Cp* analogues. Questions relating to the generality of the mechanism in Scheme 1 prompted examination of related reactions between HBCat and olefin complexes supported by the Cp complexes, Cp$_2$MH(CH$_2$═CHMe) (M ═Ta (**1a**)[18] and Nb (**1b**)[19]). Herein, we describe the results of this comparison.

Results

An isomeric mixture of *endo*- and *exo*-Cp$_2$TaH(CH$_2$═CHMe) (**1a**) and HBCat reacted to give *endo*-Cp$_2$-

---

(2) For a review of transition metal catalyzed hydroboration reported prior to 1991, see: Burgess, K.; Ohlmeyer, M. J. *Chem. Rev.* **1991**, *91*, 1179−1191.

(3) Erker, G.; Noe, R.; Wingbermuhle, D.; Petersen, J. L. *Angew. Chem., Int. Ed. Engl.* **1993**, *32*, 1213−1215.

(4) Baker, R. T.; Calabrese, J. C.; Westcott, S. A.; Marder, T. B. *J. Am. Chem. Soc.* **1995**, *117*, 8777−8784.

(5) Motry, D. H.; Smith, M. R., III. *J. Am. Chem. Soc.* **1995**, *117*, 6615−6616.

(6) Motry, D. H.; Brazil, A. G.; Smith, M. R., III *J. Am. Chem. Soc.* **1997**, *119*, 2743−2744.

(7) Sun, Y.; Piers, W. E.; Rettig, S. J. *Organometallics* **1996**, *15*, 4110−4112.

(8) Olefin complexes of Cp$_2$Ti have been postulated as intermediates in Ti-catalyzed hydroborations: He, X.; Hartwig, J. F. *J. Am. Chem. Soc.* **1996**, *118*, 1696−1702.

(9) Karl, J.; Erker, G.; Fröhlich, R.; Zippel, F.; Bickelhaupt, F.; Goedheijt, M. S.; Akkerman, O. S.; Binger, P.; Stannek, J. *Angew. Chem., Int. Ed. Engl.* **1997**, *36*, 2771−2774.

(10) This approach has proven effective for preparing iridium trisboryl complexes: Nguyen, P.; Blom, H. P.; Westcott, S. A.; Taylor, N. J.; Marder, T. B. *J. Am. Chem. Soc.* **1993**, *115*, 9329−9330.

(11) Iverson, C. N.; Smith, M. R., III *J. Am. Chem. Soc.* **1995**, *117*, 4403−4404.

(12) Lantero, D. R.; Ward, D. L.; Smith, M. R., III *J. Am. Chem. Soc.* **1997**, *119*, 9699−9708.

(13) The endo/exo designation refers to stereochemical orientations within the metallocene wedge. For the olefin complexes Cp′$_2$MH(η^2-CH$_2$═CHMe), the propylene β-C occupies the central position in the metallocene wedge in the endo isomer, while in the exo isomer the propylene β-C coordinates at an external site. Similar designations for Cp′$_2$MH$_2$BCat complexes refer to orientation of the BCat group.

(14) In this paper, "boryl" refers the generic ligand BX$_2$- whose ligation requires an increment of +1 for the formal oxidation state of the metal. A borane adduct refers to compounds where a neutral borane, HBX$_2$, is bound to the metal with η^2 coordination of the B−H bond.

(15) Lantero, D. R.; Smith, M. R., III Manuscript in preparation.

(16) Hartwig, J. F.; De Gala, S. R. *J. Am. Chem. Soc.* **1994**, *116*, 3661−3662.

(17) Lantero, D. R.; Motry, D. H.; Ward, D. L.; Smith, M. R., III *J. Am. Chem. Soc.* **1994**, *116*, 10811−10812.

(18) Klazinga, A. H.; Teuben, J. H. *J. Organomet. Chem.* **1978**, *157*, 413−419.

(19) Klazinga, A. H.; Teuben, J. H. *J. Organomet. Chem.* **1980**, *194*, 309−316.

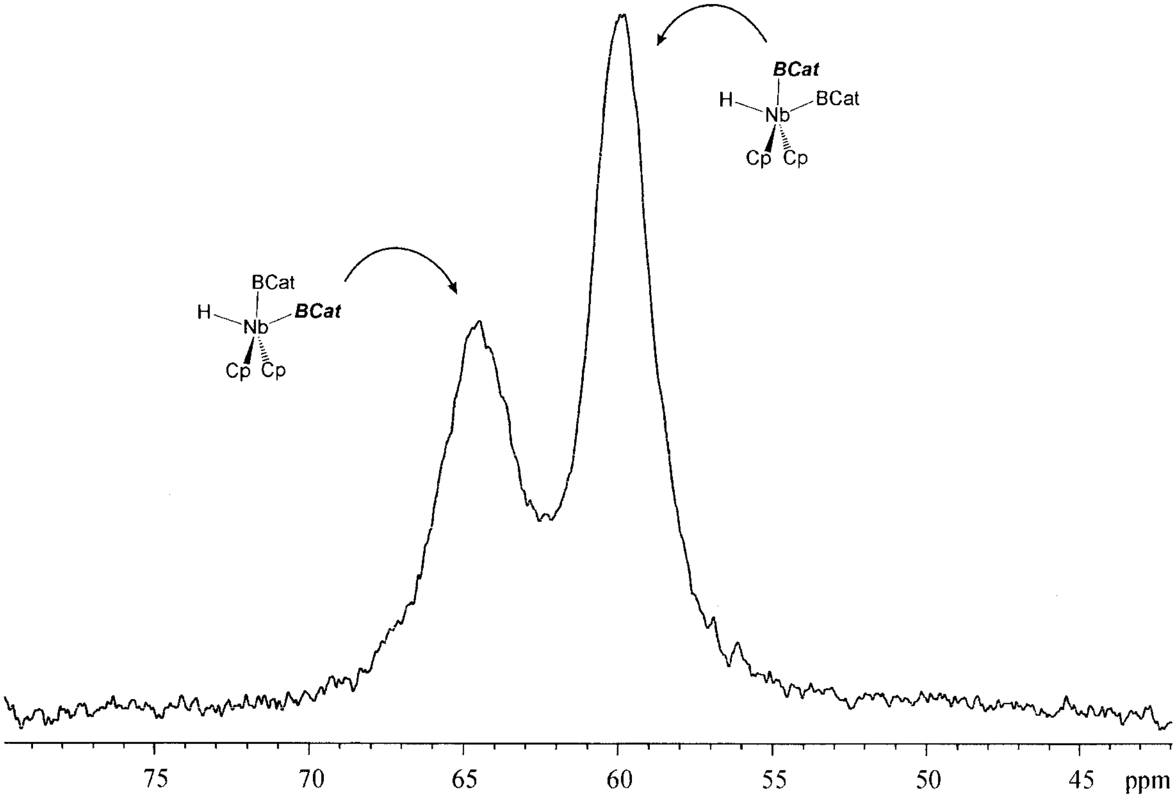

Figure 1. The ^{11}B NMR spectrum of **3** (96.2 MHz, 60 °C, C$_6$D$_6$) illustrating the chemical inequivalence of the boryl ligands. The assignment of endo and exo boryl resonances were based on isotopic labeling and ^{1}H{^{11}B} decoupling experiments.

TaH$_2$(BCat) (**2a**)[17] and *n*-PrBCat as the major products (eq 1). Although traces of the other possible boryl regioisomer, *exo*-Cp$_2$TaH$_2$(BCat),[17] were present in the reaction mixture, *endo*-**2a** could be isolated in 78% yield.

$$\underset{endo/exo\text{-}\mathbf{1a}}{endo/exo\text{-Cp}_2\text{TaH(CH}_2\text{=CHMe)}} + 2\text{HBCat} \rightarrow \underset{endo\text{-}\mathbf{2a}\text{, 78\% yield}}{endo\text{-Cp}_2\text{TaH}_2\text{(BCat)}} + n\text{-PrBCat} \quad (1)$$

When the reaction was monitored by ^{1}H NMR, the intensity of resonances assigned to *endo*-Cp$_2$TaH(CH$_2$=CHMe) diminished to the extent that *exo*-Cp$_2$TaH(CH$_2$=CHMe) was the predominant isomer in solution. When the reaction was complete, *exo*-**1a** was consumed. The analogous reaction employing DBCat gave **2a**-*d*$_{0-2}$ and *n*-PrBCat. Integration of a ^{2}H NMR spectrum gave a 40:60 ratio for deuterium incorporation in alkyl borane and the deuteride resonances of Cp$_2$TaH$_2$BCat-*d*$_{1-2}$, respectively. For the alkylborane product, the deuterium label is almost *exclusively* incorporated at the α position. When the reaction was monitored by ^{2}H NMR, exchange into the hydride positions of *exo*- and *endo*-**1a** was not detected.

An isomeric mixture of *endo*- and *exo*-Cp$_2$NbH(CH$_2$=CHMe)(**1b**) reacted with 3 equiv of HBCat to generate *n*-PrBCat, propane, propylene, Cp$_2$NbH$_2$BCat (**2b**),[16] and a new niobocene product, Cp$_2$NbH(BCat)$_2$ (**3**, eq 2). Cp$_2$NbH(BCat)$_2$ was isolated as lemon-yellow crystals in 21% yield by fractional crystallization from toluene. The ^{11}B NMR spectrum (C$_6$D$_6$, 60 °C) for compound **3** revealed two resonances at δ 65 ($\Delta\nu_{1/2}$ = 250 Hz) and δ 60 ($\Delta\nu_{1/2}$ = 210 Hz) (Figure 1). ^{1}H NMR spectra recorded between −80 and 100 °C indicated two

$$endo/exo\text{-}\mathbf{1b} + \text{xsHBCat} \rightarrow \underset{endo\text{-}\mathbf{2b}\text{, major}}{endo\text{-Cp}_2\text{NbH}_2\text{(BCat)}} + \underset{\mathbf{3}\text{, minor}}{\text{Cp}_2\text{NbH(BCat)}_2} + n\text{-PrBCat} + \text{PrH} + \text{CH}_2\text{=CHMe} \quad (2)$$

sets of chemically distinct catecholate resonances for compound **3**. A broad hydride resonance was observed at δ −7.81 ($\Delta\nu_{1/2}$ = 79 Hz), and ^{11}B decoupling experiments showed that the hydride resonance was coupled to the boron resonance at δ 60. In the IR spectrum of compound **3**, the absorption at 1651 cm^{-1} was assigned to the Nb−H stretch. The intensity of this absorption was substantially diminished in samples of **3**-*d*$_{0-1}$.

Reaction of **1b** with 2 equiv of DBCat gave **2b**-*d*$_{0-2}$, **3**-*d*$_{0-1}$, propane-*d*$_{0-2}$, and *n*-PrBCat-*d*$_{0-2}$. By integrating ^{2}H NMR spectra (C$_7$H$_8$, −20 °C), the ratio for deuterium incorporation at *n*-PrBCat, propane, and hydride positions was found to be 29:28:43. The isotopic distribution of deuterium between α, β, and γ carbons in *n*-PrBCat was 57:20:23. For propane, deuterium was preferentially incorporated at the methyl positions as the methyl and methylene resonances integrate in a 10:1 ratio. Addition of excess DBCat gave **3**-*d* as the major isotopomer. The Nb−D resonance was detected at δ −7.98 in the ^{2}H NMR spectrum of **3**-*d*. ^{11}B NMR data indicate that the resonance at δ 60 in **3**-*d* is significantly narrower ($\Delta\nu_{1/2}$ = 160 Hz) than the corresponding resonance in **3**-*d*$_0$. The Nb−D stretch was not resolved in the IR spectrum due to spectral overlap.

When the reaction between **1b** and 1 equiv of HBCat in toluene-*d*$_8$ was monitored by ^{1}H HMR, propylene and traces of propane were observed at early reaction times. In addition to Cp resonances for **2b** and **3**, new Cp (δ 4.88) and hydride resonances (δ −4.40, s, $\Delta\nu_{1/2}$ = 6 Hz and δ −6.00, $\Delta\nu_{1/2} = 64$ Hz) were detected. A NOESY spectrum revealed a cross-peak between the hydride resonances, and the $^1H\{^{11}B\}$ spectrum showed that the resonance at δ −6.00 was coupled to boron. Two new catecholate resonances were also detected at δ 7.08 and δ 6.83. The spectroscopic data are consistent with the catecholate, Cp, and hydride resonances belonging to a single intermediate, **4**, with the formula Cp_2NbH_2BCat. The ^{11}B NMR spectrum indicated a resonance at δ 59 ($\Delta\nu_{1/2} = 490$ Hz). While this may be due the boron nucleus in **4**, the shift is coincident with that of *endo*-**2b**. It has been shown that chemical shifts in Cp'_2NbH_2-BCat (Cp′ = Cp or Cp*) complexes can be insensitive to changes in the boron environment. Hence, ^{11}B chemical shifts for intermediate **4** and *endo*-**2b** could be indistinguishable.

At lower temperatures (−20 °C), a 1:1 molar ratio of HBCat and **1b** generates intermediate **4** as the major Cp-containing species (50% of integrated Cp intensity) (eq 3). Significant quantities of *endo*-**1b** (27%), *exo*-**1b** (12%), and *endo*-**2b** (11%) were also present, but the intensities of the resonances corresponding to compound **3** were insignificant. In addition to propylene, small quantities of propane were detected in the initial spectrum. The ratio between the sum of the integrations for the Cp resonances of intermediate **4** and *endo*-**2b**, and the integration for the propylene methyl resonance is approximately 10:3. The intensities of the Cp resonances for *exo*-**1b** were substantially diminished from their equilibrium values, indicating preferential propylene loss from this isomer. At longer reaction times, the intensity of the propane resonance increases and resonances for the diboryl compound, **3**, appear. At 90% conversion, the Cp resonance for compound **3** and the propane methyl resonance integrate in a 10:7.5 ratio. Similarly, the ratio between the monoboryl compound, **2b**, to compound **3** was determined to be 1.5:1. Reliable integration could not be made at higher conversion due to precipitation of compound **3**. The reaction between **1b** and 1 equiv of DBCat gives **4**-d_1 with exclusive deuterium incorporation at δ −6.21 (^2H NMR), which corresponds to the hydride resonance at δ −6.00 in the ^1H NMR spectrum. Gradually, a statistical distribution between positions corresponding to resonances at δ −4.40 and δ −6.21 is reached.

$$\textit{endo/exo}\text{-}\mathbf{1b} + \mathrm{HBCat} \xrightarrow{C_7D_8,\ -20\ °C} \underset{\mathbf{4},\ 50\%}{Cp_2NbH(\eta^2\text{-HBCat})} + CH_2{=}CHMe \quad (3)$$

Intermediate **4** persisted in solution and gradually converted to *endo*-**2b**. When *endo*-**2b** was prepared from Cp_2NbH_3 and HBCat at room temperature, resonances for intermediate **4** were not detected. However, when *endo*-**2b** was heated to 50 °C for 3 h, small quantities of **4** formed. The weak intensity for the resonances corresponding to intermediate **4** prevented accurate determination of the equilibrium constant. Intermediate **4** reacted with CO (100 psi at 25 °C) to give the carbonyl compound, $Cp_2NbH(CO)$[20] (eq 4). When the reaction was complete, the ratio between $Cp_2NbH(CO)$ and **2b** was 10:2.2, and residual *endo*-**1b** was converted to the propyl carbonyl complex, $Cp_2Nb(n\text{-}Pr)CO$.[19] Independent reactions between compounds **2b** and **3** with CO did not generate $Cp_2NbH(CO)$ under similar reaction conditions.

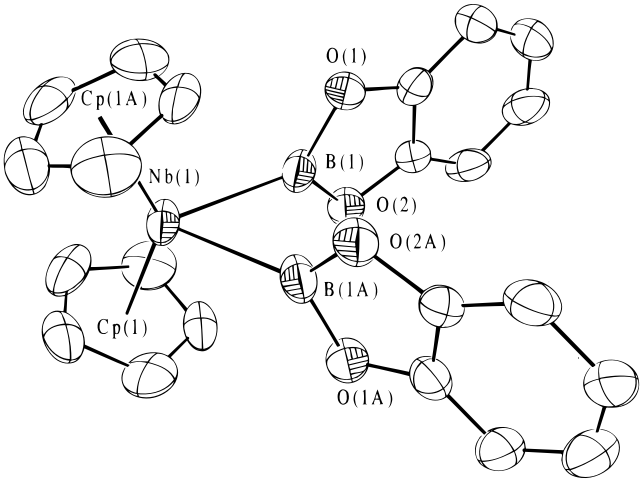

Figure 2. ORTEP diagram of $Cp_2NbH(BCat)_2$ (**3**): Nb−B = 2.29(1) Å and B(1)−Nb(1)−B(1A) = 61.1(4)°. Ellipsoids represent 50% probability for electron density. The hydride ligand could not be reliably located.

$$\underset{\mathbf{4}}{Cp_2NbH(\eta^2\text{-HBCat})} + CO \xrightarrow{C_7D_8,\ -20\ °C} \underset{82\%}{Cp_2NbH(CO)} + \mathrm{HBCat} \quad (4)$$

Single crystals of compound **3**·$Me_2C{=}O$ were grown from acetone, and its molecular structure was determined (Figure 2).[21] Systematic absences were consistent with space groups *Cc* and *C*2/*c*. Parallel refinements in both space groups converged to similar *wR2* values in both cases. However, abnormal deviations for the thermal parameters for a majority of the atoms for the *Cc* refinement suggested that the correct space group is *C*2/*c*. In this setting, the boryl ligands are symmetry related and the hydride is disordered since the Nb center lies on a C_2 axis.

Discussion

Mechanisms of olefin insertion have been thoroughly studied in group 5 metallocene systems. Significantly, the orientation of the olefin within the metallocene wedge dictates the regiochemistry of olefin insertion. For decamethylmetallocene complexes, α olefins coordinate with the α carbon exclusively residing at the exo position. When the steric requirements of cyclopentadienyl ligands are reduced, endo and exo isomers can form. Thus, endo and exo isomers give rise to primary and secondary alkyl intermediates, respectively.[22−24] After completing initial work on the reactivity of HBCat

---

[20] Otto, E. E. H.; Brintzinger, H. H. *J. Organomet. Chem.* **1978**, *148*, 29−33.

[21] We concur with a referee who stated that the stability of compound **3** in acetone is surprising. Although compound **3** eventually decomposes at room temperature in acetone, ^1H and ^{11}B NMR data for the crystals used in the X-ray experiment confirmed that decomposition had not occurred during crystallization.

[22] Doherty, N. M.; Bercaw, J. E. *J. Am. Chem. Soc.* **1985**, *107*, 2670−2682.

[23] Burger, B. J.; Santarsiero, B. D.; Trimmer, M. S.; Bercaw, J. E. *J. Am. Chem. Soc.* **1988**, *110*, 3134−3146.

[24] Green, M. L. H.; Sella, A.; Wong, L.-K. *Organometallics* **1992**, *11*, 2650−2659.

with *endo*-$Cp^*{}_2MH(CH_2{=}C(H)Me)$, we chose to investigate related chemistry of $Cp_2MH(CH_2{=}C(H)Me)$ complexes. In addition to assessing the potential for B−C bond formation involving secondary alkyl intermediates, this investigation provides a comparison between mechanisms in Cp* and Cp systems. From the results presented in this paper, it is clear that pathways for B−H activation in Cp* and Cp systems are distinct.

I. Mechanism for Ta Hydroboration. Clearly, H/D exchange occurs by some mechanism in the Ta system. Three potential mechanisms could account for the exchange, and examination of the experimental data can be used to assess the likelihood for these possibilities. First, potential hydroboration of free propylene by DBCat or transient B_2D_6 must be addressed. Either possibility should give alkylborane products with deuterium incorporation at the β positions. Therefore, α deuteration cannot be reconciled by uncatalyzed additions. Clearly, the experimental data are inconsistent with hydroboration of uncoordinated olefin.

In the second scenario, scrambling between B−D and Ta−H positions in compound **1a** could occur prior to propylene insertion into the Ta−H/D bond. Incorporation at the α position can be accounted for by B−D/Ta−H scrambling in *exo*-**1a**. Insertion of coordinated propylene into a Ta−D bond gives an isopropyl intermediate with deuterium at a methyl position. Rotation about the Ta−C bond is sufficiently rapid that β-H elimination from this intermediate will give *exo*-**1a**-d_1 with deuterium incorporation at α and γ positions. For *endo*-**1a**, propylene insertion into a Ta−D bond generates an *n*-propyl intermediate with deuterium at the β position. Subsequent β-D elimination from the propyl intermediate will regenerate the starting isotopomer with a Ta−D bond, while β-H elimination generates the Ta−H isotopomer with deuterium at the propylene β site.[25]

The previous pathway can be excluded as a significant contributor in the deuterium scrambling process. Although the small quantity of β deuterium incorporation in *n*-PrBCat-*d* could result from Ta−H/B−D exchange, this mechanism does not account for predominant incorporation at the α site since a nearly statistical distribution of the label between α and γ sites of coordinated propylene would be anticipated. Furthermore, exchange between Ta−H and B−D positions in the propylene hydride complexes should result in significant deuterium incorporation at the hydride positions in *exo*- and *endo*-**1a**. This possibility was readily tested by using ^{2}H NMR to monitor the reaction because the hydride shifts for *exo*- and *endo*-**1a** and the boryl products *endo*- and *exo*-**2a** are clearly resolved. Deuterium exchange into the hydride or propylene sites of *endo*- and *exo*-**1a** was not detected. Since selective deuterium incorporation at the α position and an absence of deuterium incorporation in *exo*- and *endo*-**1a** hydride positions cannot be reconciled by Ta−H/B−D scrambling between *exo*- and *endo*-**1a** and DBCat, this mechanism can be excluded.

The exclusive incorporation at the α position of the borane is curious, but can be reconciled by considering mechanisms that involve an alkylidene intermediate. The fact that alkylidene complexes $Cp_2Ta({=}CH_2)(CH_3)$[26] and $Cp^*{}_2TaH({=}CH_2)$[27] have been isolated supports the accessibility of $Cp_2TaH({=}CHCH_2CH_3)$ (**5**, Scheme 2). Two pathways that involve intermediate **5** could account for deuterium incorporation at the α position of *n*-PrBCat. In pathway A, B−C bond formation proceeds via σ-bond metathesis between DBCat and the Ta═C bond in intermediate **5** to give intermediate **6**. Reductive elimination from **6** generates *n*-PrBCat-d_{0-1} and Cp_2TaH-d_{0-1}, which is trapped by DBCat to give the boryl complex *endo*-**2a**.

Pathway B invokes scrambling between B−D and Ta−H sites in intermediate **5**. Reversible α migration generates a Ta propyl intermediate with deuterium incorporated in the α position. Alkylborane formation via B−H oxidative addition and subsequent B−C reductive elimination generates the Ta intermediate, Cp_2TaH/D, which is trapped by catecholborane-d_{0-1} to yield compound **2a**-d_{0-2}. For pathway B, deuterium scrambling should be reflected by diminished relative intensities for the α proton resonances of the coordinated propylene ligand in *endo*-**1a**, and it should be possible to detect HBCat by ^{11}B NMR due to the fact that $|^1J_{BH}|$ is clearly resolved for HBCat.

When the reaction between DBCat and *endo*-**1a** was monitored by ^{1}H NMR, the ratio between the integration of the α proton resonances and the Cp resonance remained constant through two half-lives. In addition, formation of HBCat could not be detected by ^{11}B NMR. These observations are inconsistent with scrambling via pathway B. Thus, the most reasonable mechanism that accounts for the isotopic incorporation is pathway A. Integration of ^{2}H NMR spectra gave a 40:60 ratio between the α-methylene resonance *n*-PrBCat and the Ta−D resonances. However, deuterium incorporation is more accurately determined by comparing α-methylene and methyl resonances in ^{1}H NMR spectra of *n*-PrBCat.[28] Since ^{2}H NMR spectra did not indicate deuterium incorporation at the methyl position of the alkylborane, the methyl resonance provides a reliable internal standard. The ratio between the α-methylene and methyl resonances (1.5:3.0) implies that the effect of k_H/k_D for reductive elimination from intermediate **6** is negligible.

II. Mechanism for Nb Boryl Production. The products from the reaction of the Nb compounds, *endo*- and *exo*-**1b**, with HBCat are distinct from those in decamethylmetallocene systems and the Ta chemistry described above. Extensive isotopic scrambling in the reaction between *endo*- and *exo*-**1b** and DBCat limits the application of labeling experiments to probe the mechanism. Nevertheless, Scheme 3 provides a rationalization for the observed products.[29] As in the decamethylmetallocene mechanism in Scheme 1, an alkyl

---

[25] β Hydrogen elimination from the intermediate $Cp_2TaH(CH_2CHDCH_3)$ will yield *endo*-$Cp_2TaH(CH_2{=}CDMe)$ while $Cp_2TaH(CH(CH_2D)CH_3)$ can give *exo*-$Cp_2TaH(CHD{=}CHCH_3)$ or *exo*-$Cp_2TaH(CH_2{=}CHCH_2D)$ upon β−H elimination.

[26] Schrock, R. R.; Sharp, P. R. *J. Am. Chem. Soc.* **1978**, *100*, 2389−2399.

[27] van Asselt, A.; Burger, B. J.; Gibson, V. C.; Bercaw, J. E. *J. Am. Chem. Soc.* **1986**, *108*, 5347−5349.

[28] Integration of the Ta deuteride and alkylborane resonances in the ^{2}H NMR spectrum gives a ratio that predicts preferential deuterium incorporation in the alkylborane. Proton incorporation that can arise from exchange of Ta−D bonds and adventitious proton sources makes integration of the ^{2}H resonances unreliable for determining the extent of deuterium incorporation in the alkylborane product. Thus, the deuterium incorporation is more accurately determined by integrating the propyl resonances in the ^{1}H spectrum of *n*-PrBCat.

Scheme 2

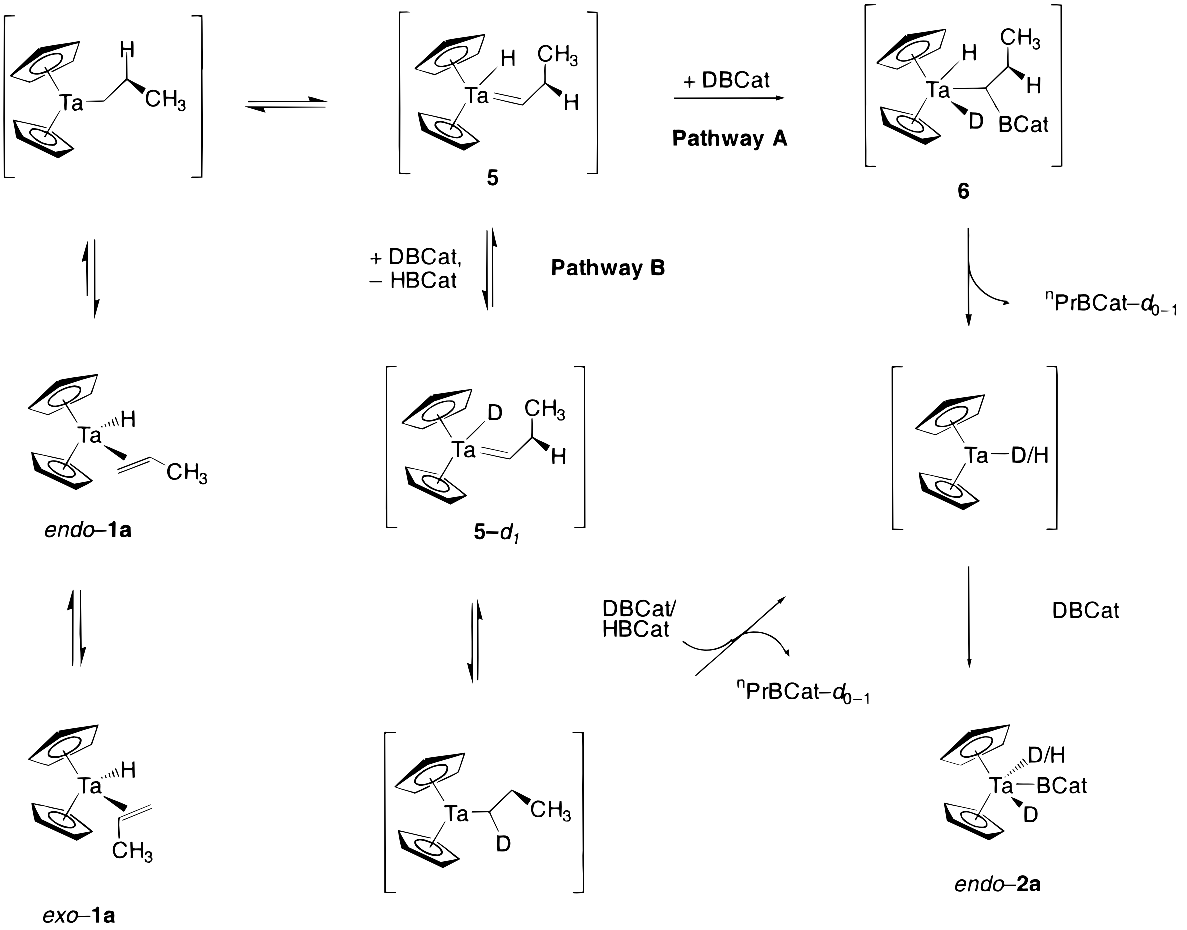

Scheme 3

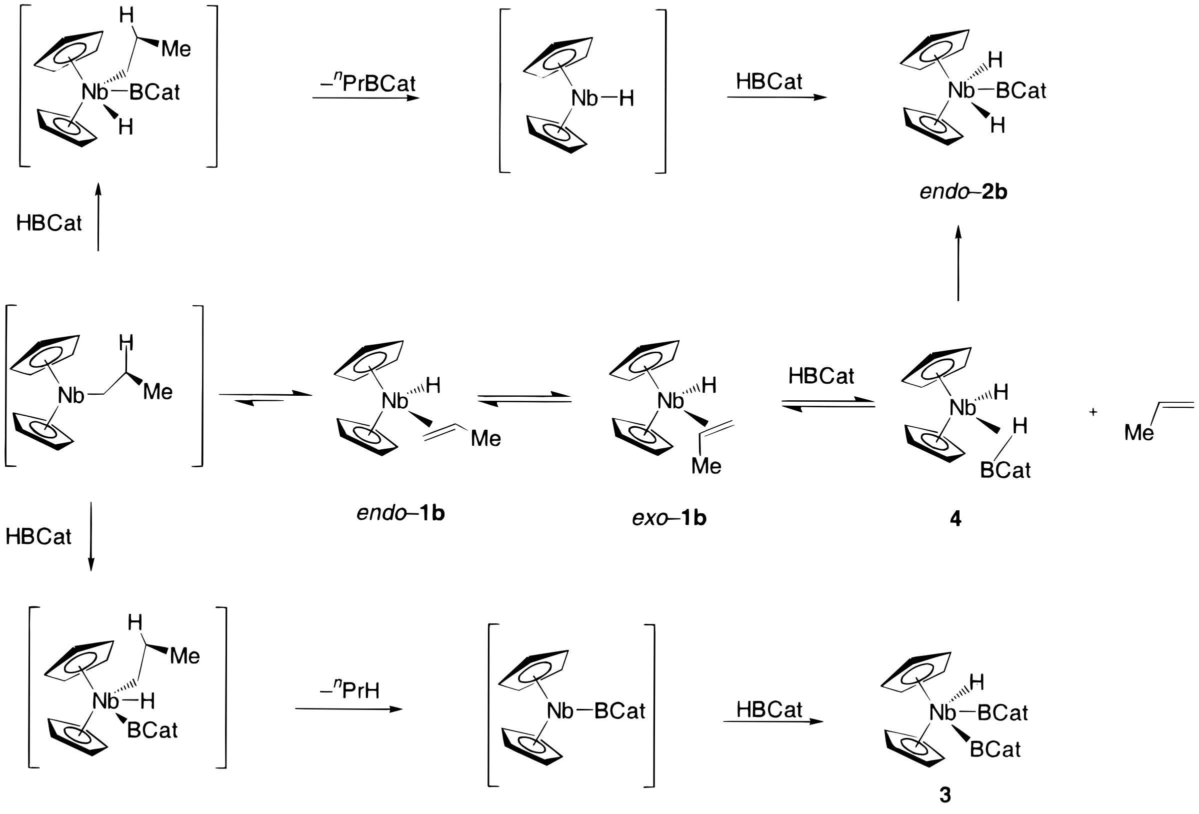

intermediate that arises from olefin insertion into the metal−hydride bond of *endo*-**1b** is invoked; however, a key difference between Schemes 1 and 3 is the orientation of the borane in the transition state corresponding to B−H activation. In Scheme 3, endo or exo orientations for the borane give rise to intermediates with the boryl group in endo or exo positions in the metallocene wedge. In Scheme 1, oxidative addition gives a single intermediate where the boryl ligand is in the endo position. The regioselectivity for B−H activation parallels that observed for olefin binding in Cp (endo or exo) and Cp* (endo) systems.

In a sequence analogous to the mechanism in Scheme 1, alkyl borane elimination from *endo*-$Cp_2NbH(n\text{-}Pr)(BCat)$ generates a hydride intermediate, which is trapped by HBCat to generate the monoboryl complex, *endo*-**2b**. This accounts for the formation of *n*-PrBCat in the reaction mixture. This event is clearly metal-mediated because the uncatalyzed of HBCat to propylene is prohibitively slow at ambient temperature. Direct conversion of intermediate **4** to *endo*-**2b** provides an alternative to the hydroboration route and accounts for the mass balance between **2b** and the sum of propylene and *n*-PrBCat concentrations.

The second B−H activation pathway generates the intermediate, *exo*-$Cp_2NbH(n\text{-}Pr)(BCat)$. Propane elimination from this isomer generates the intermediate "$Cp_2NbBCat$", which is trapped by HBCat to give the diboryl compound, **3**. The 10:7.5 ratio for the integration of the Cp protons in **3** to the methyl protons of propane was slightly higher than is predicted from Scheme 3. Two potential complications could account for the deviation from the expected 10:6 ratio. First, small quantities of propane were generated before compound **3** was detected. Second, the low solubility of compound **3** resulted in some precipitation at later reaction times. Since the solutions were cooled to give ensure dissolution of the propane, it is possible that precipitation of compound **3** was responsible for the lower ratio of compound **3** to propane. Importantly, the potential formation of compound **3** from **2b** and HBCat can be excluded since compound **3** cannot be independently prepared from compound **2b** and HBCat under similar conditions.

^1H NMR data showed that the exo isomer of **1b** reacts preferentially to form intermediate **4** and propylene. This compares with the previous observation that *exo*-**1b** reacts with CO to generate $Cp_2Nb(H)CO$ and propylene, while *endo*-**1b** reacts with CO to give the olefin insertion product, $Cp_2Nb(n\text{-}C_3H_7)CO$.[19] The mechanisms by which propylene is eliminated in reactions of compound **1b** with CO and HBCat are not necessarily similar, and future plans include a more detailed examination of these reactions.

III. Potential Structures for Intermediate 4. Recent reports have shown that boron- or silicon-containing moieties can adopt unusual geometries when bound to metal centers that also support hydride ligands.[12,16,17,30−33] Bonding in these compounds can be described in terms a continuum that is bounded by limiting valence bond structures.[16] In cases where the quality of the crystallographic data is sufficiently high, the significance of the B−H interaction can be inferred from the geometry of the metal, B, and H atoms.

Since the reliable location of hydride positions in heavy atom structures can face severe limitations, attempts have been made to probe interactions using IR and NMR spectroscopy. Although we have not successfully measured ν_{BH} for intermediate **4**, it is doubtful that the IR data would provide an unambiguous assignment of the binding mode. This is due to the fact that frequencies for M−H and M−H−B stretching modes have similar energies.[12] In principle, it may be possible to distinguish between binding modes if sufficiently high-quality calculations can reproduce experimentally determined ν_{BH} and ν_{MH} values. Since we presently do not have this information, we have resorted to characterizing intermediate **4** by NMR spectroscopies.

Isotopic perturbation of equilibrium resulting from deuterium substitution has been extensively applied in NMR studies of equilibria involving hydrogen transfer.[34−36] For two rapidly equilibrating species, isotopic substitution shifts the equilibrium as a result of the difference between H and D zero-point energies. Since the observed chemical shift is the average of limiting shifts for the equilibrating structures, perturbation in equilibrium results in variations of observed chemical shifts for different isotopomers. It is crucial to recognize that large chemical shift differences have been attributed exclusively to intrinsic isotope effects.[37] Thus, a large chemical shift difference is not rigorously diagnostic for structural equilibration. If the chemical shift of a resonance in question is temperature independent, exclusive contributions from intrinsic isotope effects could account for the observed shift. Hence, temperature-dependent chemical shifts provide stronger evidence for equilibrium origins when large isotopic shifts are observed.

The isotopic perturbation of equilibrium that results from deuterium substitution has been applied by Hartwig and co-workers to probe B−H interactions in *endo*-**2b**-d_{0-2}.[16] Equilibrium between boryl and borohydride structures was invoked to account for consecutive upfield shifts of hydride and deuteride resonances upon deuterium substitution. Temperature dependence for the chemical shift perturbation was not demonstrated in this study.[38] Thus, chemical shift differences arising from intrinsic isotope effects cannot be excluded. A related example involving equilibrium between Ir di-

---

(29) Although B−H activation in Scheme 3 is depicted as proceeding through oxidative addition/reductive elimination sequences, a mechanism predicated on σ bond metathesis is also plausible.

(30) Luo, X.-L.; Kubas, G. J.; Bryan, J. C.; Burns, C. J.; Unkefer, C. J. *J. Am. Chem. Soc.* **1994**, *116*, 10312−10313.

(31) Spaltenstein, E.; Palma, P.; Kreutzer, K. A.; Willoughby, C. A.; Davis, W. M.; Buchwald, S. L. *J. Am. Chem. Soc.* **1994**, *116*, 10308−10309.

(32) Hartwig, J. F.; Muhoro, C. N.; He, X.; Eisenstein, O.; Bosque, R.; Maseras, F. *J. Am. Chem. Soc.* **1996**, *118*, 10936−10937.

(33) Muhoro, C. N.; Hartwig, J. F. *Angew. Chem., Int. Ed. Engl.* **1997**, *36*, 1510−1512.

(34) Saunders, M.; Telkowski, L.; Kates, M. R. *J. Am. Chem. Soc.* **1977**, *99*, 8070−8071.

(35) Saunders, M.; Kates, M. R. *J. Am. Chem. Soc.* **1977**, *99*, 8071−8072.

(36) The vibrational theory that governs intrinsic isotope effects has been reviewed: Jameson, C. J.; Osten, H. J. *Annu. Rep. NMR Spectroscop.* **1986**, *17*, 1.

(37) Isotopic shifts that were previously attributed to perturbation of equilibrium have been convincingly shown to arise from intrinsic isotope effects: Balzer, H. H.; Berger, S. *J. Phys. Org. Chem.* **1997**, *10*, 187−189.

(38) Shifts as large as 78 ppb have been attributed to intrinsic isotope effects in Ir hydride complexes: Heinekey, D. M.; Millar, J. M.; Koetzle, T. F.; Payne, N. G.; Zilm, K. W. *J. Am. Chem. Soc.* **1990**, *112*, 909−919.

hydrogenhydride/trihydride species has been recently reported by Heinekey and co-workers.[39] In this study, the evidence for chemical shift differences arising from isotopic perturbation of equilibrium is more convincing. In addition to the temperature-dependent shifts for the H_3, H_2D, and HD_2 isotopomers, temperature-dependent $|J_{HT}|$ values for tritiated compounds correlate with equilibrium constants extracted from the chemical shift data.

For group 5 metallocene complexes with H and BCat ligands in the coordination sphere, large chemical shift differences from isotopic substitutions arise when B−H interactions are present.[12,16,17] Spectroscopic data for structurally characterized compounds show no obvious correlation between binding mode (borylhydride vs borane adduct) and magnitude or direction of the isotopic shift, which limits interpretations based on isotopic probes. Although it is not clear whether the observed shifts arise from perturbation of equilibrium or intrinsic isotope effects in group 5 metallocene complexes, isotopic labeling experiments for intermediate **4** yield data that can be directly compared to spectroscopic data of closely related compounds, which have been structurally characterized.

Although we have not successfully isolated intermediate **4**, we can generate sufficient concentrations of this species to collect relevant spectroscopic data. Since $^1H\{^{11}B\}$ spectra prove that the resonance at −6.00 ppm is coupled to boron, formulations for intermediate **4** require two chemically inequivalent hydride resonances, one of which is boron coupled. Potential structures that satisfy this requirement are shown below (**4A**−**D**). Structures **A** and **B** are borane adducts of Cp_2NbH, structure **C** is the Nb(V) analogue of the Ta compound, *exo*-**2a**, and structure **D** is an O-bound borane adduct of Cp_2NbH.

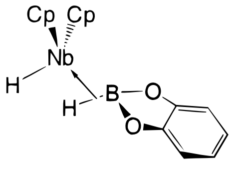

A

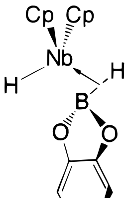

B

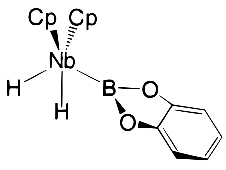

C

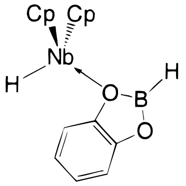

D

Isomer **D** can be excluded for the following three reasons. First, two resonances are assigned to the catecholate protons in intermediate **4**. Four chemically inequivalent resonances would be expected for the aromatic protons in **D**.[40] Second, $|J_{HB}|$ should be similar to that in catecholborane; however, the coupling in intermediate **4** is not resolved. Third, the high-field shift for the proton coupled to boron is typical for a compound with a metal hydride interaction and atypical for a three-coordinate dialkoxyborane.

Distinguishing between the remaining possibilities is more difficult. The ease with which borane is eliminated from intermediate **4** compares favorably with borane eliminations from borane adducts and contrasts the reactivity of group 5 boryl complexes. This circumstantial evidence suggests formulation as a borane adduct (**A** or **B**). A closer examination of the spectroscopic data provides a more rigorous determination.

Since **C** is analogous to the structurally characterized Ta compound, *exo*-**2a**, it should exhibit spectroscopic similarities.[17] Figure 3 shows ^1H and $^1H\{^{11}B\}$ spectra for intermediate **4** and *exo*-**2a**. The chemical shifts for the hydride ligands, and the magnitude of the isotopic perturbation for the upfield resonance, parallel those in compound *exo*-**2a**. The only disparity between the spectroscopic data for intermediate **4** and compound *exo*-**2a** is that $|^2J_{HH}|$, which is clearly resolved in compound *exo*-**2a** ($|^2J_{HH}| = 5.6$ Hz), is unresolved for intermediate **4**. This difference is significant since similar $|^2J_{HH}|$ values for Cp_2MH_3 (M = Nb, 9−11 Hz;[41,42] M = Ta, 10 Hz[43]) predict that $|^2J_{HH}|$ should be resolved for structure **C**. In Cp_2NbH_3, normal magnetic coupling is masked by exchange coupling, which has equal magnitude and opposite sign at certain temperatures.[42] The fact that $|^2J_{HH}|$ was not resolved in spectra from −60 to 20 °C ensures that $|^2J_{HH}|$ is not similarly obscured for intermediate **4**. On the basis of these observations, isomer **C** can be discounted.

Having eliminated isomers **C** and **D**, the formulations that are most consistent with the spectroscopic data are **A** and **B**. The cross-peak between the hydride resonances that is observed in the NOESY spectrum of intermediate **4** could arise from nuclear Overhauser effects or chemical exchange. The latter possibility can be rigorously eliminated since exclusive deuterium incorporation at δ −6.21 in the ^2H NMR spectrum of **4**-*d* proves that exchange is slow on the NMR time scale. The NOESY data are consistent with some contribution from **A**, but a cross-peak between the hydride resonances would also be expected if equilibrium between **A** and **B** were rapid on the NMR time scale.

The 200 ppb upfield shift of the B-coupled deuteride resonance in intermediate **4** raises the possibility of equilibrium between structures **A** and **C**. Variable-temperature NMR experiments indicate small variations in the chemical shifts for the resonances in Figure 3a. However, the hydride chemical shifts do not vary linearly with temperature as was found for Ir dihydrogenhydride/trihydride equilibria.[39,44] If contributions from isomer **C** to the spectrum of intermediate **4** are significant, two-bond coupling between the hydride ligands should be observed. Since $|^2J_{HH}|$ cannot be

---

[39] Oldham, W. J.; Hinkle, A. S.; Heinekey, D. M. *J. Am. Chem. Soc.* **1997**, *119*, 11028−11036.

[40] A process that rapidly exchanges coordinated and uncoordinated oxygen atoms would give two resonances. This exchange would not effect arguments based on $|^1J_{HB}|$, chemical shift, or isotope effects on chemical shifts.

[41] Curtis, M. D.; Bell, L. G.; Butler, W. M. *Organometallics* **1985**, *4*, 701−707.

[42] Heinekey, D. H. *J. Am. Chem. Soc.* **1991**, *113*, 6074−6077.

[43] Deutsch, P. P.; Maguire, J. A.; Jones, W. D.; Eisenberg, R. *Inorg. Chem.* **1990**, *29*, 686−690.

[44] The high-field resonance shifts from δ −5.98 (−50 °C) to −6.04 (0 °C) and the low-field resonance shifts from δ −4.36 (−50 °C) to −4.39 (0 °C). From 0 to 50 °C, the low-field resonance approaches a limiting value of δ −4.40.

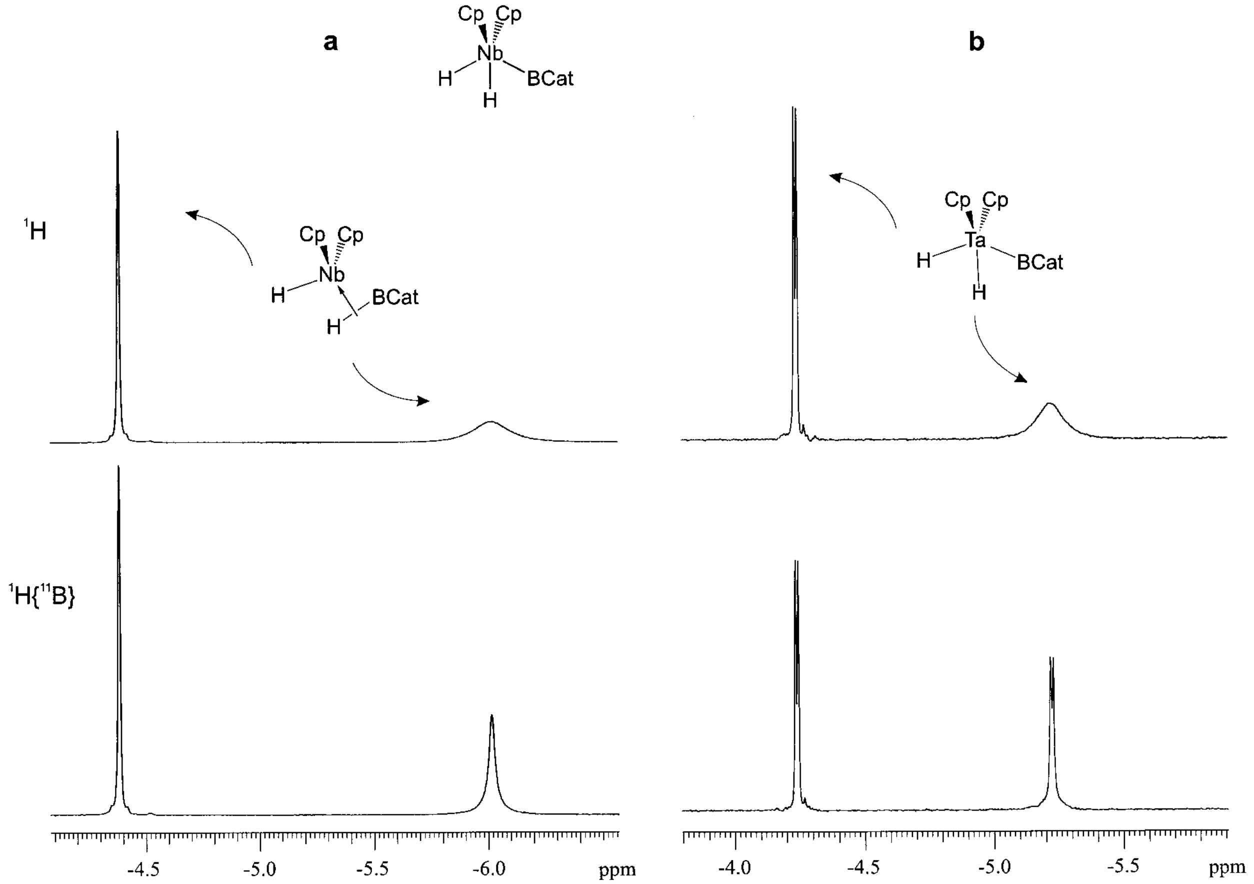

Figure 3. ^1H and $^1H\{^{11}B\}$ spectra for (a) intermediate **4** (500 MHz, C_7D_8, −20 °C) and (b) *exo*-**2a** (500 MHz, C_6D_6, 20 °C).

resolved in spectra of intermediate **4** at any temperature, the temperature-dependent shifts for the hydride resonances cannot be conclusively attributed to an equilibrium between **A** and **C**.

Given that there is no evidence for an equilibrium between isomers **A** and **B**, and the NOESY data support an interaction between the hydride ligands, we favor the exo structure, **A**, for intermediate **4**. The irreversible conversion of intermediate **4** to *endo*-**2b** suggests a mechanism involving isomerization of **A** to **B**, followed by B−H oxidative addition. It is not clear whether the rate-limiting step should be isomerization or oxidative addition. This could be difficult to probe experimentally; however, evaluation of putative reaction coordinates by computational methods could provide some mechanistic insight.

IV. Structural and Spectroscopic Features of Compound 3. Compound **3** joins a relatively small family of structurally characterized diboryl complexes.[11,45−51] The fact that the spectroscopic data for **3** indicate chemically distinct boryl units initially suggests that the three ligands in the metallocene wedge would adopt a typical geometry for a Cp_2MX_3 compound, such as that found for Cp_2NbH_3.[52] The chemically distinct boryl environments are accounted for if one boryl ligand occupies the endo position of the wedge with the remaining boryl and hydride ligands being constrained to exo positions in the metallocene wedge. This situation contrasts the bonding in niobocene and tantalocene disilylhydride complexes, where the silyl ligands are chemically equivalent and occupy exo positions in the metallocene wedge.[53,54] Despite the fact that the hydride position is not resolved in the crystal structure for compound **3**, the possibility that the hydride bridges the boron atoms can be excluded since resonances corresponding to a single BCat environment would be expected in ^1H and ^{11}B NMR spectra. The crystallographic equivalence of the boryl ligands in compound **3** was not anticipated, and it is somewhat surprising that the presence of an adjacent hydride ligand apparently has no structural consequences.

---

(45) Baker, R. T.; Calabrese, J. C.; Westcott, S. A.; Nguyen, P.; Marder, T. B. *J. Am. Chem. Soc.* **1993**, *115*, 4367−4368.

(46) Nguyen, P.; Lesley, G.; Taylor, N. J.; Marder, T. B.; Pickett, N. L.; Clegg, W.; Elsegood, M. R. J.; Norman, N. C. *Inorg. Chem.* **1994**, *33*, 4623−4624.

(47) Hartwig, J. F.; He, X. *Angew. Chem., Int. Ed. Engl.* **1996**, *35*, 315−317.

(48) Ishiyama, T.; Matsuda, N.; Murata, M.; Ozawa, F.; Suzuki, A.; Miyaura, N. *Organometallics* **1996**, *15*, 713−720.

(49) Lesley, G.; Nguyen, P.; Taylor, N. J.; Marder, T. B.; Scott, A. J.; Clegg, W.; Norman, N. C. *Organometallics* **1996**, *15*, 5127−5154.

(50) Dai, C.; Stringer, G.; Corrigan, J. F.; Taylor, N. J.; Marder, T. B.; Norman, N. C. *J. Organomet. Chem.* **1996**, *513*, 273−275.

(51) Dai, C.; Stringer, G.; Marder, T. B.; Baker, R. T.; Scott, A. J.; Clegg, W.; Norman, N. C. *Can. J. Chem.* **1996**, *74*, 2026−2030.

(52) Wilson, R. D.; Koetzle, R. F.; Hart, D. W.; Kvick, Å.; Tipton, D. L.; Bau, R. *J. Am. Chem. Soc.* **1977**, *99*, 1775−1781.

(53) Several tantalum disilyl complexes with the formula *endo*-$Cp_2Ta(SiR_3)_2H$ were prepared in this study. For $SiR_3 = SiMeH_2$, *endo*-$Cp_2Ta(SiMeH_2)_2H$ was detected as the minor isomer: Jiang, W.; Carroll, P. J.; Berry, D. H. *Organometallics* **1991**, *10*, 3648−3655.

(54) Interestingly, the reaction of **2b** with $HSiMe_2Cl$ gives the symmetric complex $Cp_2NbH(SiMe_2Cl)_2$ where the silyl groups occupy the exo positions. A nonclassical Si−H−Si interaction was proposed on the basis of chemical shift data and the X-ray structure. NMR data were consistent with chemically equivalent silyl ligands: Nikonov, G. I.; Kuzmina, L. G.; Lemenovskii, D. A.; Kotov, V. V. *J. Am. Chem. Soc.* **1995**, *117*, 10133−10134.

The quality of the diffraction data for compound **3** was marginal. After the final least-squares cycle, the most intense peak in the difference map was located 1.06 Å from B(1) and 1.51 Å from Nb(1). The peak is oriented exo to the B(1) and B(1A) positions and lies near the plane defined by Nb(1), B(1), and B1(A).[55] We do not believe that the location of this peak is a reliable indication of the true hydride position since marginal quality of the data set is further exacerbated by the C_2 crystallographic symmetry at Nb that reduces the hydride intensity to half the normal value. The heavy atom positions are more precisely determined. Hence, the Nb−B distance and the B(1)−Nb−B(1A) angle in compound **3** merit comparison to values in related structures.

The Nb−B distance (2.29(1) Å) compares to M−B distances in *endo*-**2b** Nb (2.292(5) Å) and *exo*- and *endo*-**2b** (*exo*-**2a**, Ta−B = 2.295(11); *endo*-**2a**, Ta−B 2.263(6) Å).[16,17] The Nb−B distance is shorter than M−B distances in the borane adducts, $Cp^*_2Nb(H_2BO_2C_6H_3$-4-*t*-Bu) (Nb−B = 2.348(4) Å)[12] and $Cp_2Ti(HBCat)_2$ (Ti−B = 2.335(5) Å).[32] The B(1)−Nb(1)−B(1A) angle (61°) in **3** is considerably smaller than the B−W−B angle (78°) in $Cp_2W(BO_2C_6H_3$-3,5-*t*-Bu$)_2$,[56] and approaches the value for B−Ti−B angle (54°) in the Ti borane adduct, $Cp_2Ti(HBCat)_2$. The B−Ti−B angle in $Cp_2Ti(HBCat)_2$ is more acute than those typically found in d^2 Cp_2MX_2 species; however, the authors noted that the angle formed by the midpoints of the B−H vectors and the Ti center (81°) falls within the range of those measured for d^2 Cp_2MX_2 compounds.[57] Since the hydride location in compound **3** is poorly defined, an analogous argument cannot be reliably applied to compound **3**.[58]

Recent studies have shown B−H interactions in catecholateboryl complexes do not require rehybridization at boron. To determine whether interactions between the hydride and boryl ligands were present in compound **3**, $^1H\{^{11}B\}$ spectra were measured and spectroscopic data for $Cp_2NbH(BCat)_2$ and $Cp_2NbD(BCat)_2$ were compared. Selective boron-decoupling experiments showed that the hydride is coupled to the boron resonance at δ 60 (Figure 1). This permits the unambiguous assignment of the ^{11}B spectrum and indicates that a B−H interaction is present in compound **3**. The isotopic shift for the hydride resonance (180 ppb) is also consistent with significant B−H interactions in compound **3**. The magnitude is similar to isotopic shifts in compounds *endo*-**2b** and *exo*-**2a**, where B−H interactions are present, and substantially larger than isotopic shifts in *endo*-**2a**, where B−H interactions are absent. The chemical shift for the hydride resonance was temperature independent between −80 and 25 °C (^1H NMR, 300 MHz, THF-d_8).[59]

Two limiting valence bond descriptions that are consistent with B−H interactions inferred from the spectroscopic data are shown below. Isomer **E** is a borane adduct of Nb^{III}, where borane coordination is similar to that observed in $Cp_2Ti(HBCat)_2$ and $Cp^*_2Nb(H_2BCat)$. Isomer **F** is a boryl hydride structure that compares to *exo*-**2a** and *endo*-**2b**. The spectroscopic data clearly illustrate limitations of inferences based solely on crystallographic data for compound **3**. Specifically, ^1H and ^{11}B NMR spectra clearly show that the boron environments are chemically distinct, which contrasts the crystallographic symmetry that requires equivalent boron positions. Since the hydride chemical shift is temperature independent, the possibility that the isotopic shift arises from isotopic perturbation of equilibrium between structures **E** and **F** is unlikely.

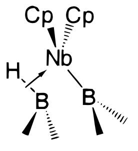

E

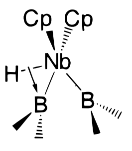

F

We examined the chemical reactivity of compound **3** to determine whether its behavior was more consistent with formulation **E** or **F**. The borane adducts, $Cp_2Ti(HBCat)_2$ and $Cp^*_2Nb(H_2BCat)$, eliminate borane readily to generate borane trapping products $Cp_2Ti(CO)_2$ and $Cp^*_2NbH(CO)$ when CO is present. Under similar conditions, HBCat elimination from the boryl complexes *exo*- and *endo*-$Cp_2TaH_2(BCat)$ and *endo*-$Cp_2NbH_2(BCat)$ is prohibitively slow. When the reaction between compound **3** and CO (100 psi, 50 °C, 12 h) was examined, $Cp_2NbH(CO)$ and HBCat were not detected.

Additional information regarding potential elimination reactions is provided by ^1H and ^{11}B NMR data. There is no evidence for boron site exchange via a symmetrical intermediate arising from B−H reductive elimination/oxidative addition since coalescence of BCat resonances is not observed (eq 5). Rapid HBCat reductive elimination and stereospecific B−H oxidative addition, shown in eq 6, would not lead to coalescence; however, this possibility can be eliminated by the fact that chemical shifts for the BCat resonances are not perturbed when HBCat is added to solutions of compound **3**.

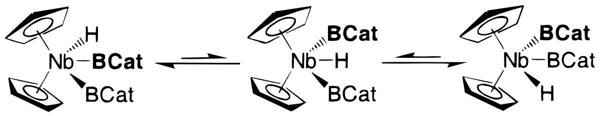

(5)

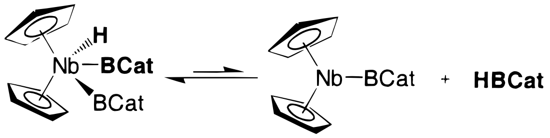

(6)

---

[55] There was no significant electron density located between B(1) and B(1A).

[56] Hartwig, J. F.; He, X. *Organometallics* **1996**, *15*, 5350−5358.

[57] Prout, K.; Cameron, T. S.; Forder, R. A. *Acta Crystallogr. B* **1974**, *30*, 2290−2304.

[58] Using an average estimate for an Nb−H distance (1.65 Å), and the extrema for B−H distances in catecholate complexes where B−H interactions are significant, the estimated range for the angle defined by the midpoint of the B−H vector, Nb, and the exo boryl ligand is 80 $> \theta >$ 74. This value is typical for a d^2 complex and smaller than the range for X-M-X angles in d^0 complexes (94−97°). Clearly this comparison suffers from the ill-defined hydride position in compound **3**. Furthermore, the electronic-based argument neglects potential steric contributions, and the inherent asymmetry in compound **3** may limit direct comparison to $Cp_2Ti(\eta^2$-$HBCat)_2$.

[59] A conceivable, but unlikely, scenario could lead to temperature-independent shifts for equilibrating structures. If entropic contributions to ΔG for structures **E** and **F** (or any other equilibrating structures) are identical, or the limiting hydride chemical shifts for different structures are coincident, the equilibrium could be temperature dependent.

We favor valence bond description **F** for two reasons. First, the Nb−B bond distance is similar to M−B bond distances in other group 5 boryl complexes and shorter than M−B distances in borane adducts of Nb and Ti. For structure **E**, we would anticipate that the Nb−B in compound **3** would be similar to those for d^2 Nb and Ti complexes. Second, we do not observe borane elimination chemistry that we would expect for isomer **E**. Although correlations between structure and reactivity of complexes with the generic formulas $Cp'_2MH_x(BCat)_{3-x}$ (x = 1, 2) can be rationalized in valence-bond terms, there are obvious limitations to applying valence bond models in systems with three-center/two-electron interactions.

Conclusions

The results from the present study highlight mechanistic diversity for reactions of HBCat with olefin hydride complexes of the formula, $Cp'_2MH(CH_2{=}CHMe)$ (Cp′ = Cp, Cp*; M = Nb, Ta). Although the products obtained in the reaction between $Cp_2TaH(CH_2{=}CHMe)$ and HBCat are analogous to those observed in related reactions of decamethylmetallocene complexes, data from isotopic labeling studies suggest that B−C bond-forming pathways in Cp_2M and Cp^*_2M (M = Nb and Ta) systems are different. Specifically, results from the present investigation are consistent with B−H activation by alkylidene intermediates for the Cp_2Ta derivatives, whereas previous studies implicated B−H activation by alkyl intermediates in Cp* systems.

The products formed from the reaction of *exo*- and *endo*-$Cp_2NbH(CH_2{=}CHMe)$ with HBCat are unique. The formation of propane and the diboryl compound, **3**, suggests that B−H activation in this system can give intermediates with boron in the exo position of the metallocene wedge. This deviates from the exclusive formation of alkylborane and *endo*-$Cp^*_2MH_2BCat$ products for Cp* derivatives. Presumably, the increased steric demand of the Cp* ligand prevents exo approach of the BCat group, whereas endo and exo approaches are possible for the less hindered Cp ligand.

The exo isomer of $Cp_2NbH(CH_2{=}CHMe)$ is the only $Cp'_2MH(CH_2{=}CHMe)$ derivative that reacts via olefin *loss* to give a complex with the formula Cp'_2MH_2BCat. The spectroscopic features for intermediate **4** have been compared to related compounds that have been structurally characterized. The structure that is most consistent with the data is the Nb^{III} complex, *exo*-$Cp_2NbH(\eta^2\text{-}HBCat)$. Chemical behavior of intermediate **4** is consistent with this description as facile HBCat elimination parallels reactivity of other borane adducts.

The spectroscopic and structural data for the compounds in the present work expands the database for $Cp'_2MH_x(BCat)_{3-x}$ (x = 1, 2) derivatives. The large isotope effects for deuteride chemical shifts observed for **3**-*d* and **4**-d_1 have magnitudes similar to those previously reported for *endo*-**2b** and *endo*-$Cp^*_2Nb(H_2BCat)$. The spectroscopic data for compounds **3** and **4** suggests that the isotopic shifts may result from large intrinsic isotope effects for hydrides that interact with BCat ligands. The application of computational methods to provide a deeper understanding of the bonding and spectroscopic features in these systems is desirable.

Experimental Section

General Considerations. All manipulations were performed using glovebox, Schlenk and vacuum-line techniques. Pentane, heptane, THF, and toluene were predried over sodium. Toluene was distilled from Na/benzophenone ketyl. Acetone was dried over activated 3 Å molecular sieves and distilled prior to use. All other solvents were distilled from sodium/benzophenone ketyl. Benzene-d_6 and toluene-d_8 were dried over activated 3 Å molecular sieves and then vacuum transferred into a sodium-mirrored container. THF-d_8 was dried over activated 3 Å molecular sieves and then vacuum transferred prior to use. Argon and nitrogen gases were purified by passage over MnO on silica.

Catecholborane (Aldrich) was vacuum transferred prior to use. Preparation of catecholborane-*d* was accomplished by reacting $NaBD_4$ (Aldrich) and $BF_3{\cdot}OEt_2$ (Mallinckrodt) to produce BD_3 which was then bubbled through a THF solution of catechol (Aldrich). The THF was then distilled from the solution at atmospheric pressure, and the remaining solution was vacuum distilled to give the borane as a clear, viscous liquid. Ethylene (Matheson) and propylene (Matheson) were subjected to several freeze−pump−thaw cycles and then transferred in vacuo to reaction vessels. CO (AGA Gas Inc.) was used as received. $Cp_2NbH(C_2H_4)$,[60] *exo*- and *endo*-$Cp_2NbH(C_3H_6)$,[19] and *exo*- and *endo*-$Cp_2TaH(C_3H_6)$[18] were prepared by literature methods. The *exo*- and *endo*-$Cp_2TaH(C_3H_6)$ mixture was prepared by irradiating pure *endo*-$Cp_2TaH(C_3H_6)$ with 300 nm light for 4 h under an atmosphere of propylene gas generating 41% *exo*-$Cp_2TaH(C_3H_6)$ and 59% *endo*-$Cp_2TaH(C_3H_6)$.

^1H NMR spectra were recorded on Varian Gemini-300 (300.0 MHz), Varian VXR-300 (299.9 MHz), and Varian VXR-500 (499.9 MHz) spectrometers and referenced to residual proton solvent signals. ^2H NMR spectra were recorded on a Varian VXR-300 spectrometer operating at 46.0 MHz or a Varian VXR-500 spectrometer operating at 76.7 MHz; spectra were referenced to residual deuterium signals of the solvent. ^{11}B NMR spectra were recorded using a Varian VXR-300 spectrometer operating at 96 MHz or a Varian VXR-500 spectrometer operating at 160 MHz, and spectra were referenced to a $BF_3{\cdot}Et_2O$ external standard solution. Infrared spectra were recorded as Nujol mulls between KBr plates using a Nicolet IR/42 spectrometer.

Procedures. *endo*-$Cp_2TaH_2(BO_2C_6H_4)$ (*endo*-2a). Catecholborane (800 mg, 6.8 mmol) was dissolved in 10 mL of toluene and then added via cannula to a 100-mL toluene solution of *endo*-$Cp_2TaH(C_3H_6)$ (950 mg, 2.7 mmol). The solution was stirred for 2 h during which time the color gradually darkened to dark yellow. The solvent was then reduced until a light-yellow microcrystalline solid precipitated from solution. The solution was then placed in a −15 °C freezer. After 12 h, the supernatant was removed by filtration, and the yellow microcrystals were dried under vacuum (915 mg, 78%): mp 141−143 °C (dec); ^1H NMR (C_6D_6) δ 7.15 (m, 2H, $O_2C_6H_4$), 6.83 (m, 2H, $O_2C_6H_4$), 4.85 (s, 10H C_5H_5), −4.23 (s, 1H, TaH);^{11}B NMR (C_6D_6) δ 70.0 ($\Delta\nu_{1/2}$ = 250 Hz); IR (cm^{-1}) 1751 (ν_{TaH}).

$Cp_2NbH(BO_2C_6H_4)_2$ (3). A 5-mL toluene solution of catecholborane (250 mg, 2.1 mmol) was added to a 5-mL toluene solution of *exo*- and *endo*-$Cp_2NbH(C_3H_6)$ (190 mg, 0.71 mmol) at room temperature, and the resulting solution was stirred overnight at room temperature. The solution gradually changed to an orange-red, and a yellow solid precipitated from solution. The solids were then allowed to settle, and the filtrate was removed via cannula. The solids were then washed with cold toluene and vacuum-dried. The product was isolated as yellow microcrystals (68 mg, 21%): mp 178−181 °C (dec); ^1H NMR

---

(60) Lichtenberger, D. L.; Darsey, G. P.; Kellogg, G. E.; Sanner, R. D.; Young, V. G., Jr.; Clark, J. R. *J. Am. Chem. Soc.* **1989**, *111*, 5019−5028.

(C_6D_6) δ 7.00 (m, 2H, $O_2C_6H_4$), 6.93 (m, 2H, $O_2C_6H_4$), δ 6.63 (m, 2H, $O_2C_6H_4$), 6.57 (m, 2H, $O_2C_6H_4$), 5.11 (s, 10H C_5H_5), -7.71 (br, 1H, Nb*H*); ^{1}H NMR (THF-d_8) δ 6.89 (m, 2H, $O_2C_6H_4$), 6.82 (m, 2H, $O_2C_6H_4$), 6.69 (m, 2H, $O_2C_6H_4$), 6.66 (m, 2H, $O_2C_6H_4$), 5.59 (s, 10H C_5H_5), -7.81 (br, 1H, Nb*H*); ^{11}B NMR (C_6D_6, 60 °C) δ 65 ($\Delta\nu_{1/2} = 250$ Hz), δ 60 ($\Delta\nu_{1/2} = 210$ Hz); IR (cm^{-1}) 1651 (ν_{NbH}).

$Cp_2NbD(BO_2C_6H_4)_2$. A 10-mL toluene solution of $Cp_2NbH(C_2H_4)$ (550 mg, 2.2 mmol) was added to catecholborane-*d* (1.0 g, 8.7 mmol). The resulting solution was stirred overnight at room temperature. The solution gradually changed to orange-red, and during the course of the reaction a yellow solid precipitated from solution. The solids were then allowed to settle, and the filtrate was removed via cannula. The solids were then washed with cold toluene. The product was isolated as yellow microcrystals (263 mg, 26%): ^{1}H NMR (THF-d_8) δ 6.85 (m, 2H, $O_2C_6H_4$), 6.77 (m, 2H, $O_2C_6H_4$), δ 6.66 (m, 2H, $O_2C_6H_4$), 6.62 (m, 2H, $O_2C_6H_4$), 5.55 (s, 10H C_5H_5); ^{2}H NMR (THF) δ −7.98 (br, Nb*D*); ^{11}B NMR (C_6D_6, 60 °C) δ 65 ($\Delta\nu_{1/2} =$ 220 Hz), δ 60 ($\Delta\nu_{1/2} = 160$ Hz).

NMR Tube Reactions. *exo*- and *endo*-$Cp_2TaH(C_3H_6)$ + Catecholborane. A 21-mg (0.059 mmol) sample of *exo*- and *endo*-$Cp_2TaH(C_3H_6)$ was dissolved in benzene-d_6 along with catecholborane (15 mg, 0.12 mmol). The resulting solution was placed in a NMR tube and flame sealed. An immediate ^{1}H NMR demonstrated that *endo*-$Cp_2TaH(C_3H_6)$ is used preferentially at early reaction times with the formation of only one set of alkylborane resonances with predominant formation of *endo*-$Cp_2TaH_2(BO_2C_6H_4)$ and slight formation of *exo*-$Cp_2TaH_2(BO_2C_6H_4)$. Only *exo*-$Cp_2TaH(C_3H_6)$ remained (44% of the original *exo*-$Cp_2TaH(C_3H_6)$ present) upon standing at room temperature for 12 h in the dark. Another ^{1}H NMR spectrum, taken after the tube was heated at 40 °C for 2.5 h, revealed one set of alkylborane resonances, *endo*-$Cp_2TaH_2(BO_2C_6H_4)$ (84%) and *exo*-$Cp_2TaH_2(BO_2C_6H_4)$ (16%), with no detection of *exo*-$Cp_2TaH(C_3H_6)$.

***endo*-$Cp_2TaH(C_3H_6)$ + Catecholborane-*d*.** A 12-mg (0.035 mmol) sample of *endo*-$Cp_2TaH(C_3H_6)$ was dissolved in 0.6 mL of toluene along with 8 mg of catecholborane-*d* (0.07 mmol), and the solution was placed in an NMR tube. The resulting solution was allowed to react for several hours at room temperature. A ^{2}H NMR spectrum was recorded. Deuterium incorporation was witnessed only the hydride position of the *endo*-**2b** and the α carbon position of *n*-PrBCat. Integration of the ^{2}H NMR spectrum revealed 40% of the deuterium label was located in the alkyl borane and 60% of the label was located in the hydride position of the tantalum boryl complex.

***endo*-$Cp_2TaH(C_3H_6)$ + Catecholborane-*d*.** *endo*-$Cp_2TaH(C_3H_6)$ (12 mg, 0.034 mmol) was dissolved in 0.6 mL of toluene-d_8 along with 8 μL of catecholborane-*d* (0.07 mmol), and the solution was placed in an NMR tube. The resulting solution was allowed to react at room temperature for several hours. Integration of the *n*-PrBCat alkyl resonances resulted in the ratio between α, β, and γ protons as 1.5:2:3.

Generation of Intermediate 4. *exo*- and *endo*-$Cp_2NbH(C_3H_6)$ (20 mg, 0.076 mmol) was dissolved in 0.6 mL of toluene-d_8, and the solution was placed in a J-Young NMR tube. Catecholborane (9 μL, 0.08 mmol) was added to the headspace of the NMR tube. The NMR tube was kept horizontal to prevent mixing of the reagents. Upon removal from the glovebox, the NMR tube was immediately placed in a dry ice/2-propanol bath. Once the tube had been cooled, the contents of the NMR tube were allowed to mix. The reaction was monitored at −20 °C: ^{1}H NMR (toluene-d_8) δ 7.08 (m, 2H, $O_2C_6H_4$), 6.83 (m, 2H, $O_2C_6H_4$), 4.88 (s, 10H C_5H_5), −4.40 (s, 1H, Nb*H*), −6.00 (br, 1H, Nb*H*); ^{11}B NMR (toluene-d_8) δ 59 ($\Delta\nu_{1/2} = 490$ Hz). A NOESY spectrum revealed a cross-peak between the two hydride positions of the intermediate.

***exo*- and *endo*-$Cp_2NbH(C_3H_6)$ + Catecholborane-*d*.** A 23-mg (0.085 mmol) sample of *exo*- and *endo*-$Cp_2NbH(C_3H_6)$ was dissolved in 0.6 mL of toluene, and the solution was added to a J-Young NMR tube. Catecholborane-*d* (10 μL, 0.08 mmol) was added to the headspace of a J-Young NMR tube which was then capped. The tube was kept horizontal to prevent mixing of the two reagents. Upon removal from the glovebox, the tube was immediately cooled in a dry ice/2-propanol bath. The contents of the NMR tube were allowed to react at −20 °C as periodic ^{2}H NMR spectra were recorded. Exclusive deuterium incorporation was observed at the high-field resonance of intermediate **4** (^{2}H NMR δ −6.21) at early reaction times. A gradual mixing of the deuterium label was seen between the two hydride positions of intermediate **4** over 12 h at room temperature (^{2}H NMR δ −4.42 and −6.21)

In a separate experiment, *exo*- and *endo*-$Cp_2NbH(C_3H_6)$ (10 mg, 0.039 mmol) was loaded into a J-Young NMR tube. A solution of catecholborane-*d* (10 mg, 0.078 mmol) in 0.6 mL of toluene was then added to the NMR tube. The resulting NMR sample was quickly capped and kept at room temperature for 6 h. A ^{2}H NMR spectrum revealed the formation of **2b**-d_{0-2}, **3**-d_{0-1}, propane-d_{0-2}, and *n*-PrBCat-d_{0-2}. The ratio for deuterium incorporation at *n*-PrBCat, propane, and hydride positions was found to be 29:28:43 by integration of ^{2}H NMR spectra (C_7H_8, −20 °C). The isotopic distribution of deuterium between α, β, and γ carbons in *n*-PrBCat was 57:20:23. For propane, deuterium was preferentially incorporated at the methyl positions as the methyl and methylene resonances integrate in a 10:1 ratio.

***exo*- and *endo*-$Cp_2NbH(C_3H_6)$ + Catecholborane + CO.** An 18-mg (0.067 mmol) sample of *exo*- and *endo*-$Cp_2NbH(C_3H_6)$ was dissolved in 0.6 mL toluene-d_8, and the solution was placed in a high-pressure NMR tube. Catecholborane (8 μL, 0.07 mmol) was then added to the headspace of the NMR tube which was sealed with a Teflon plug. The tube is maintained as close to horizontal as possible to prevent a reaction from immediately occurring. The tube is immediately placed in a dry ice/2-propanol bath upon removal from the glovebox. Once the toluene solution was cooled, the contents of the tube were allowed to react at −20 °C for 30 min. A ^{1}H NMR (−20 °C) was then taken to ensure the intermediate complex had formed. The tube was then again placed in a dry ice/2-propanol bath and pressurized to 100 psi with CO. The contents of the tube were allowed to warm to room temperature. A ^{1}H NMR taken at 25 °C revealed the formation of $Cp_2NbH(CO)$[20] as the major product along with *endo*-**2b** and compound **3**.

Crystal Structure Determination and Refinement for 3. Data were collected at 173 K on a Rigaku AFC6S diffractometer using Mo Kα radiation ($\lambda = 0.710\ 69$ Å). Final unit cell parameters were obtained by least-squares refinement of 25 reflections that had been accurately centered. Three standard reflections were recorded after every 150 scans, with no significant change in intensity noted. The structures were solved using SHELX-86. Atomic coordinates and thermal parameters were refined using the full-matrix least-squares program, SHELXL-93, and calculations were based on F^2 data. All non-hydrogen atoms were refined using anisotropic thermal parameters. All crystallographic computations were performed on Silicon Graphics Indigo computers.

Lemon yellow crystals of $Cp_2NbH(BO_2C_6H_4)_2$ (fw 461.5) were grown from a concentrated acetone solution cooled to −80 °C. The crystals were coated with Paratone-N, and a suitable crystal was selected and mounted on a glass fiber. Compound **3** crystallized in a monoclinic crystal system with systematic absences indicating the space group *C*2/*c* (No. 15) with the following cell parameters: $a = 15.585(6)$ Å, $b = 13.789(9)$ Å, $c = 12.701(7)$ Å, $\beta = 120.86(3)°$, $V = 2343(2)$ Å^3, $Z = 4$; density (calcd) = 1.309 mg/cm^3. The 2029 independent reflections were collected between $4.0 \leq 2\theta \leq 50.0°$ using $\omega/2\theta$ scans.

All non-hydrogen atoms were found using SHELXS-86. The hydrogen atoms of the cyclopentadienyl ring and the boryl catecholate ring were placed in calculated positions and refined independently without restraints. Full-matrix least-squares refinement on F^2 (2029 data, 0 restraints, 184 parameters) converged to give the following values: $R1 = 0.0547$, $wR2 = 0.1430$, GOF = 1.075 for $[I > 2\sigma(I)]$. For all data: $R1 = 0.1172$, $wR2 = 0.1798$. $R1 = \Sigma(F_o^2 - F_c^2)/\Sigma F_o^2$, $wR2 = [(w(F_o^2 - F_c^2)^2/\Sigma w(F_o^2)^2)]^{1/2}$, and GOF $= (\Sigma(|F_o^2| - |F_c^2|)/\sigma)/(n - m)$ where $w = 1/\sigma^2 (F_o^2)$, n is the number of reflections used, and m is the number of variables.

Acknowledgment. The NMR equipment was provided by the National Science Foundation (CHE-8800770) and the National Institutes of Health (1-S10-RR04750-01). We thank the administrators of the ACS Petroleum Research Fund, the Exxon Educational Foundation, and the National Science Foundation (CHE-9520176) for support of this work. We thank the referees whose suggestions led to significant improvement of the final manuscript.

Supporting Information Available: X-ray data for compound **3** (13 pages). Ordering information is given on any current masthead page.

OM980908M